Annals of Anatomy 260 (2025) 152670

Contents lists available at ScienceDirect

Annals of Anatomy

journal homepage: www.elsevier.com/locate/aanat

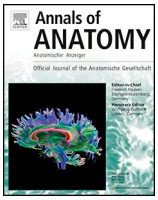

Effect of isolated keratin 3 knockdown on gene expression of primary limbal epithelial cells without and with inflammatory stimuli

Swarnali Kundu [a,*], Maryam Amini [a], Tanja Stachon [a], Fabian Fries [a,b], Berthold Seitz [b], Zhen Li [a], Shuailin Li [a], Shanhe Liu [a], Shao-Lun Shu [a], Shweta Suiwal [a], Nóra Szentmáry [a]

[a] Dr. Rolf M. Schwiete Center for Limbal Stem Cell and Congenital Aniridia Research, Saarland University, Homburg, Saar, Germany
[b] Department of Ophthalmology, Saarland University Medical Center, Homburg, Saar, Germany

ARTICLE INFO

Keywords:
Keratin 3
KRT3
PAX6
Congenital aniridia
Limbal epithelial cells

ABSTRACT

Purpose: Studies have shown that keratin 3 (KRT3) expression is reduced in paired box 6 (PAX6) haploinsufficient primary limbal epithelial cells (LECs). The downregulation of KRT3 expression due to PAX6 haploinsufficiency is likely a critical factor in the development and progression of aniridia associated keratopathy (AAK). In addition, the ocular surface of congenital aniridia patients exhibits an inflammatory environment. The objective of this study was to investigate the isolated effect of KRT3 knockdown, achieved via siRNA silencing in healthy LECs, on PAX6 and other related gene expressions, both under normal and inflammatory conditions.
Methods: To achieve KRT3 knockdown, human primary LECs were transfected with KRT3 siRNA using Lipofectamine 2000. Inflammatory conditions were induced 48 hours after transfection by treating the cells with 2 mg/mL of lipopolysaccharides (LPS) or 1 ng/mL of IL-1β. Subsequently, gene and protein expression levels were analysed using qPCR, Western blotting, and ELISA.
Results: Following KRT3 knockdown at protein level, there was DSG1, ADH7 and PPARγ upregulation and MAPK1 downregulation solely at transcriptional level ($p \leq 0.031$). Nevertheless, IL-6 downregulation could be observed both at transcriptional and at protein levels ($p \leq 0.003$). Following KRT3 siRNA knockdown, LPS induced inflammation decreased PPARγ mRNA level and IL-1β induced inflammation decreased DSG1 and ADH7 mRNA levels without changes at protein levels ($p \leq 0.014$). In contrast, in control knockdown LECs, IL-1β induced inflammation significantly decreased KRT3 mRNA and protein levels and IL-6 protein level ($p \leq 0.02$).
Conclusions: In normal LECs, inflammatory stimuli slow differentiation and simultaneously induce IL-6 production. These mechanisms are absent in KRT3 knockdown LECs. As a result, despite the presence of inflammation, KRT3 knockdown LECs continue their differentiation unaltered while maintaining inflammatory IL-6 protein secretion.

1. Introduction

PAX6 is a key transcription factor in human eye development, influencing nearly all anatomical structures of the eye. PAX6 haploinsufficiency leads to a rare condition known as congenital aniridia, or PAX6 syndrome. Most congenital aniridia patients exhibit iris hypoplasia, progressive aniridia-associated keratopathy (AAK), progressive limbal stem cell deficiency (LSCD), secondary glaucoma, congenital and juvenile cataracts, as well as optic nerve head and macular hypoplasia (Ihnatko et al., 2022).

PAX6 isoforms regulate several genes, including those involved in the expression of corneal epithelial keratins. Studies have shown that keratin 3 (KRT3) and keratin 12 (KRT12) expression is reduced in PAX6 haploinsufficient primary limbal epithelial cells (LECs) (Latta et al., 2018b). Overexpression studies further reveal that PAX6 promotes KRT3 expression, while the PAX6(5a) isoform specifically induces KRT12 expression (Katiyar et al., 2022; Szaflik et al., 2008; Li et al., 2008; Ouyang et al., 2014; Cunha et al., 2019). PAX6 is known to preserve corneal epithelial identity and stability by regulating differentiation markers such as KRT3 and KRT12 (Katiyar et al., 2022; Kitazawa et al., 2017; Thaya Ramaesh et al., 2003; K. Ramaesh et al., 2005). The downregulation of KRT3 and KRT12 expression due to PAX6 haploinsufficiency is likely a critical factor in the development and progression of AAK. Cytokeratins or keratins are a sub-family of cytoskeletal

* Corresponding author.
E-mail address: s8swkund@uni-saarland.de (S. Kundu).

https://doi.org/10.1016/j.aanat.2025.152670
Received 21 February 2025; Received in revised form 25 April 2025; Accepted 1 May 2025
Available online 5 May 2025

Table 1
Age and gender of the donors used.

Donors	Gender	Age (Years)
Donor 1	Male	60
Donor 2	Male	70
Donor 3	Male	73
Donor 4	Female	80
Donor 5	Female	80
Donor 6	Male	86

proteins, that are localised in the intracytoplasmic cytoskeleton of epithelial cells. Cytokeratins are widely recognized as markers of epithelial cells and are expressed in well-defined phases during epithelial development and differentiation (Mall et al., 1982). KRT3/KRT12 is specifically expressed in corneal epithelial cells as heterodimers. Additionally, keratins are also used as tumour markers for diagnostic purposes (Karantza, 2011; Kiselev et al., 2018).

Limbal epithelial stem cells (LESCs) are undifferentiated compared to the central corneal epithelium and lack the cytokeratin markers (Latta et al., 2018b). Nevertheless, in patients with PAX6 haploinsufficiency and congenital aniridia, there is a progressive loss of the limbal epithelial cell niche (Schlötzer-Schrehardt et al., 2021). LESCs play a crucial role in maintaining corneal epithelial turnover and giving rise to LECs (Sasamoto et al., 2016). From the limbus to the central epithelium, as LESCs differentiate, the expression of KRT3 and KRT12 gradually increases, helping to preserve the integrity and stability of the central corneal epithelium (Cao et al., 2013; Chen et al., 2015; Kao et al., 1996). Since keratins are essential for the structural functionality of the corneal epithelium, and PAX6 can bind to the KRT3 promoter, studying the isolated effect of KRT3 knockdown in healthy donor cells via siRNA knockdown is of interest. This includes evaluating its impact on PAX6 and other associated genes, such as KRT12.

KRT3 (GeneID #3850; OMIM #148043) and KRT12 (GeneID #3859; OMIM #601687) are clustered in a region of chromosome 12q12-q13. Mutations in these genes have been implicated in Meesmann epithelial corneal dystrophy (MECD), first reported by Irvin et al. in 1997 (Irvine et al., 1997). The absence of KRT3 and KRT12 in MECD is characterised by fragile corneal epithelium, identifiable morphologically by vacuolated intraepithelial cysts (Irvine et al., 1997). Consequently, certain epithelial cell properties in MECD may share similarities with those observed in PAX6 haploinsufficient congenital aniridia.

Studies have revealed that the ocular surface of congenital aniridia patients exhibits an inflammatory environment, and a distinct protein profile compared to healthy individuals. The tears of aniridia patients are rich in cytokines, such as eotaxin, and contain various interleukins, including IL-1β, IL-9, and IL-17A, as well as other inflammation-enhancing molecules like macrophage inflammatory protein 1α (MIP-1α/CCL3) and basic fibroblast growth factor (bFGF/FGF2)(Landsend et al., 2018; Ihnatko et al., 2013; Simmons et al., 2016). To replicate the inflammatory ocular surface environment observed in aniridia patients, we designed experiments that simulate similar inflammatory conditions. The use of lipopolysaccharides (LPS) (Page et al., 2022) and interleukin-1β (IL-1β) (Primiani et al., 2014) to induce inflammation in cell culture systems is a well-established and widely applied method in biomedical research. Reported effective ranges for LPS are 1–10 μg/mL, and for IL-1β, 0.5–10 ng/mL (Yücel et al., 2017; Dias and Banerjee, 2013; Reeve et al., 2000).

Our aim was to investigate the isolated effect of KRT3 knockdown in healthy donor LECs via siRNA knockdown on the expression of PAX6 and other associated genes, both under normal and inflammatory conditions.

2. Material and methods

2.1. Ethical considerations

Our study was approved by the Ethical Committee of Saarland/ Germany (no. 162/23). In all the experiments described henceforth, the human donor tissues were handled according to the Declaration of Helsinki principles.

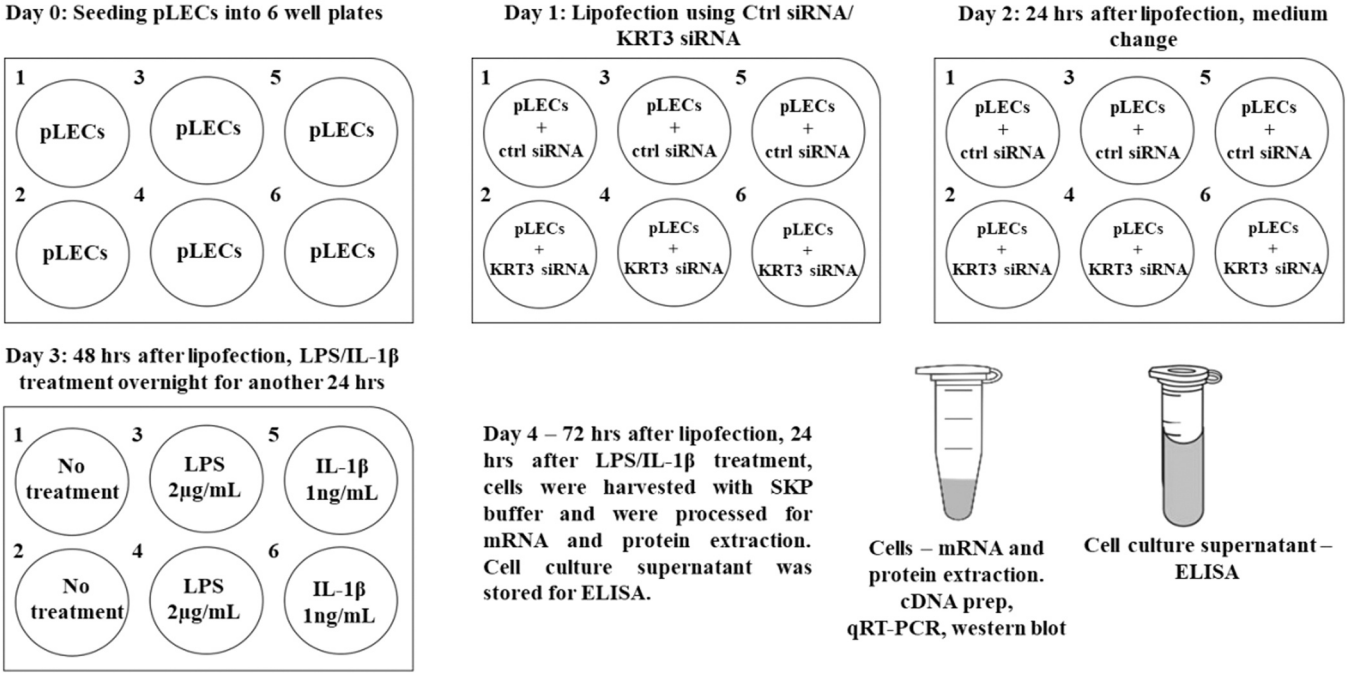

Fig. 1. The experimental workflow was annotated day-by-day, starting from day 0. An animated workflow illustrates our experimental set-up, including the handling and treatment of human primary limbal epithelial cells (pLECs). Seventy-two hours after lipofection with either control (Ctrl) or KRT3 siRNA knockdown (KRT3 siRNA), and 24 hours after inflammatory treatment [lipopolysaccharides (LPS) or interleukin 1β (IL-1β)], the cells were harvested for mRNA, and protein extraction. The extracted mRNA was used for downstream processes, such as cDNA preparation. Additionally, the supernatant from each condition was collected for analysis using ELISA.

Table 2
Qiagen QuantiTect™ primer pairs used for qPCR.

Target mRNA transcript	Catalogue No.	Amplicon size (bp)
ADH7: NM_000673, NM_001166504	QT00000217	85 bp
ALDH3A1: NM_000691	QT0240193	121 bp
CRABP2: NM_001199723, NM_001878, XM_006711169	QT00063434	140 bp
DSG1: NM_001942	QT00001617	96 bp
FABP5: NM_001444	QT00225561	97 bp
FOSL2: NM_005253, XM_005264231, XM_006711976, XM_006711977	QT01000881	117 bp
IL−6: NM_000600, XM_005249745	QT00083720	107 bp
KRT3: NM_057088	QT00050365	118 bp
KRT12: NM_000223	QT00011949	104 bp
KRT13: NM_002274, NM_153490	QT00068747	60 bp
KRT19: NM_002276	QT00081137	117 bp
MAPK1: NM_002745, NM_138957	QT00065933	118 bp
MAPK3: NM_001109891, NM_002746	QT02589314	187 bp
MMP2: NM_004530	QT02395778	95 bp
NF-kB: (RELA 2): (NM_001243984, NM_001243985, NM_001145138, NM_021975)	QT02324308	136 bp
PAX6: NM_000280, NM_001127612, NM_001604, NM_001258462, NM_001258463, NM_001258464, NM_001258465	QT00071169	113 bp
PPARγ: NM_005037, NM_015869, NM_138711, NM_138712, XM_006713208	QT00029841	113 bp
TBP: NM_001172085, NM_003194	QT00000721	132 bp
VEGA: NM_001025366, NM_001025367, NM_001025368, NM_001033756, NM_001171623, NM_001171624, NM_001171625, NM_001171626, NM_001171629, NM_003376, NM_001287044	QT01010184	273 bp

2.1.1. Culturing primary LECs, in vitro

Primary LECs cultures were prepared, as described previously (Katiyar et al., 2022; Lorenz Latta et al., 2019). In short, LECs were obtained from corneoscleral rims provided by the Klaus Faber Center for Corneal Diseases, including the Lions Eye Bank, following their use in corneal transplantation. Briefly, the limbal region was excised using a 1.5 mm biopsy punch (PFM Medical AG, Köln, Germany), and the tissue fragments were incubated overnight at 37°C with 5 % CO_2 in a solution of 0.5 mg/mL Collagenase A (Roche Pharma AG, Basel, Switzerland).

Primary human LECs were isolated by excising the upper half-depth of the corneal limbal region under light microscopy. The tissue was incubated at 37°C for 24 hours in keratinocyte growth medium (KGM3, PromoCell GmbH, Heidelberg, Germany) supplemented with 1 mg/mL collagenase A (Roche Diagnostic GmbH, Mannheim, Germany, No.10103578001). Following lysis, the tissue was treated with trypsin-EDTA (0.05 % trypsin/0.02 % EDTA, Sigma-Aldrich® GmbH, Geisenheim, Germany) to detach cells. The suspension was centrifuged at 800 × g for 4–5 minutes at room temperature, and the cell pellet was resuspended in KGM3 before seeding into 6-well culture plates with 2.5 mL KGM3 per well.

Cultures were maintained in an incubator at 37°C with 95 % relative humidity and 5 % CO_2, with the medium replaced every 2–3 days. Trypsinization was employed to eliminate limbal fibroblasts, ensuring a purity of > 95 % limbal epithelial cells. Cells were expanded and subcultured until achieving 80 % confluence in all six wells. Only primary LECs at passages P2–P4 with appropriate confluence were used for experiments. The age and gender of the donors included in this study are presented in Table 1.

2.1.2. siRNA transfection of LECs, and inflammatory treatment

The LECs were deemed optimal for transfection when monolayer confluency reached 60 %. At this stage, LECs were seeded onto 6-well cell culture plates (Greiner Bio-One GmbH, Frikenhausen, Germany) and were subjected to siRNA transfection. All experiments utilized LEC cultures between the first and second passages.

Control LECs were transfected with 150 pmol of non-specific control siRNA (Catalogue no. #4390843, Thermo Fisher Scientific, Silencer™ Select Negative Control, Waltham, USA). For KRT3 knockdown, primary LECs were transfected with 150 pmol of KRT3 siRNA (5'->3': sense strand: AGAUGAGAUCGACUUCUUA, antisense strand: UAAGAA-GUCGAUCUCAUCU; Catalogue no. #4392420, Thermo Fisher Scientific, Silencer™ Select KRT3, Waltham, USA).

First, for each well, 150 pmol (1.5 µl of 100 pmol/µl) of siRNA oligonucleotide was diluted in 250 µl of Opti-MEM™ (1X) + GlutaMAX™ (Gibco, USA). Additionally, in a second tube, 7.5 µl of Lipofectamine™ 2000 Transfection Reagent (Thermo Fisher Scientific, California, USA) was diluted in 250 µl of Opti-MEM™ (1X) + GlutaMAX™ and incubated for 5 minutes. The contents of the first and second tubes were combined and incubated for 20 minutes. Then, this volume, was supplemented by 2 mL of Keratinocyte Growth Medium (KGM3), added to each of the 6 wells.

Twenty-four hours after transfection, the medium was replaced with fresh supplemented KGM3. After 48 hours, inflammatory conditions were simulated by supplementing fresh medium with lipopolysaccharides (LPS) or interleukin (IL)-1β. Since primary human LECs are more susceptible to stress and damage compared to immortalized cell lines, we chose lower-end concentrations to ensure a balance between inflammatory activation and cell viability. In our study, we selected 2 µg/mL of LPS and 1 ng/mL of IL-1β based on concentrations demonstrated in prior literature to effectively stimulate an inflammatory response without causing cytotoxic effects (Dias and Banerjee, 2013; Page et al., 2022; Primiani et al., 2014; Reeve et al., 2000; Yücel et al., 2017). Specifically, 2.5 µl of LPS (Sigma-Aldrich, Israel) at a final concentration of 2 µg/mL per well or 0.25 µl of IL-1β (Peprotech, USA) at a final concentration of 1 ng/mL per well was added to the respective treatment wells.

The experimental workflow is summarized in Fig. 1. In summary, the following treatment condition pairs were established:

1–2) Control siRNA/KRT3 siRNA knockdown.

3–4) Control siRNA/KRT3 siRNA knockdown +LPS treatment at 2 µg/mL per well.

5–6) Control siRNA/KRT3 siRNA knockdown+IL-1β treatment at 1 ng/mL per well.

Up to 96–120 hours after initial seeding onto six-well culture plates, corresponding to 72 hours post-transfection and 24 hours after induction of inflammatory treatment, morphologically, the primary human limbal epithelial cells maintained a typical cobblestone appearance characteristic of a healthy epithelial monolayer, and no morphological changes were observed following the inflammatory stimulus. The cell culture supernatants and the cell lysates were collected 72 hours after transfection. Cell lysates were collected using SKP buffer supplied with the RNA/DNA/Protein Purification Plus Micro Kit (Norgen, Thorold, ON, Canada, Catalogue no. 47700).

2.2. RNA/Protein extraction and cDNA -synthesis

RNA and protein were extracted from the cell lysates of the specified cell cultures using the RNA/DNA/Protein Purification Plus Micro Kit (Norgen, Thorold, ON, Canada, Catalogue no. 47700), following the standardized manufacturer protocol for primary cells. RNA concentration was measured using UV/VIS spectrophotometry (ScanDrop, Analytic Jena, Jena, Germany). Protein concentration was determined using a standardized Bradford assay (Sigma-Aldrich GmbH, USA) with a spectrophotometric plate reader (Infinite50, TECAN, Zurich, Switzerland).

cDNA synthesis was carried out using the OneTaq RT-PCR Kit (New England Biolabs, Frankfurt a.M., Germany). For the first strand of cDNA synthesis, 1000 ng of RNA was used per reaction with M-MuLV Enzyme Mix and oligo(dT) primers (OneTaq RT-PCR Kit, NEB) in a total reaction

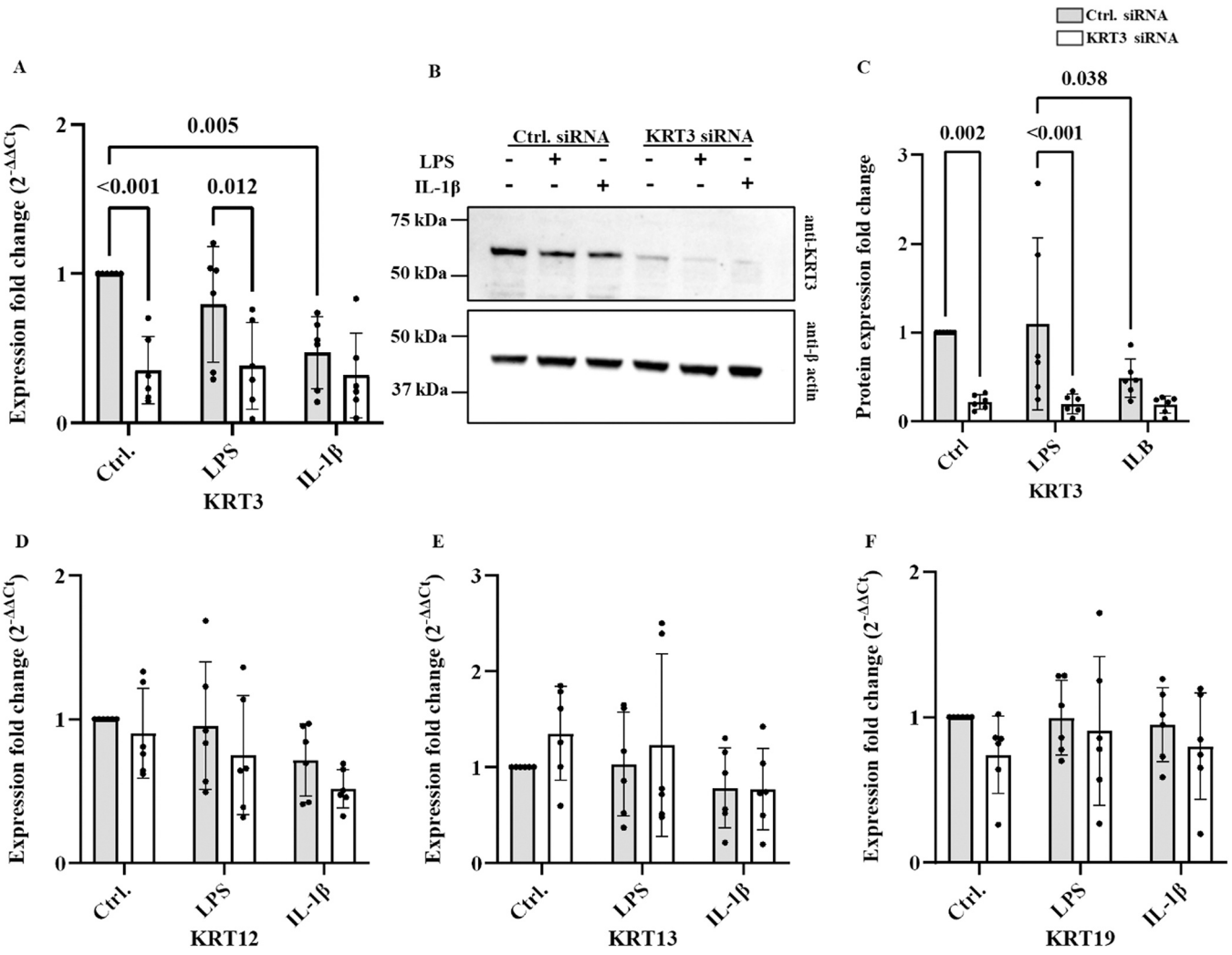

Fig. 2. Keratin 3 (KRT3) mRNA and protein and keratin 12 (KRT12), keratin 13 (KRT13) and keratin 19 (KRT19) mRNA levels in primary human limbal epithelial cells (LECs) 72 hours after transfection with control siRNA (grey) or with KRT3 knockdown siRNA (white), without or with lipopolysaccharide (LPS) or interleukin 1β (IL-1β) treatment (n = 6) (A-F). Data are shown as mean ± SD. Statistical analysis has been performed using two-way ANOVA followed by Tukey test. Representative western blot images are also displayed (B). p values below 0.05 were considered statistically significant. KRT3 mRNA levels were significantly lower following KRT3 siRNA knockdown, compared to siRNA controls, both in the absence and presence of LPS-induced inflammation ($p \leq 0.0120$). Similarly, KRT3 protein levels were significantly reduced after KRT3 siRNA knockdown compared to siRNA controls, with and without LPS-induced inflammation ($p \leq 0.002$). Additionally, KRT3 mRNA levels were significantly lower in IL-1β-induced inflammation in control siRNA-transfected cells compared to non-inflamed conditions ($p = 0.005$). KRT3 protein levels were also significantly lower in IL-1β-induced inflammation compared to LPS-induced inflammation in control siRNA-transfected cells ($p = 0.038$). In contrast, KRT12, KRT13, and KRT19 mRNA levels did not show significant changes following KRT3 siRNA knockdown, regardless of LPS or IL-1β treatment ($p \geq 0.085$).

volume of 20 µl. Prior to use, 30 µl of nuclease-free water was added to each tube.

2.3. Quantitative polymerase chain reaction (qPCR)

For the qPCR reaction, the following components were added to each well of a 96-well plate (MicroAmp™ Optical Reaction Plate, Applied Biosystems, USA): 1 µl of cDNA, 1 µl of primer, 3 µl of nuclease-free water, and 5 µl of ACEq DNA SYBR Green Master Mix (Vazyme Biotech, Nanjing). The qPCR experiments were performed in technical duplicates using the QuantStudio™ thermocycler (Thermo Fisher Scientific, USA). Qiagen QuantiTect™ primers were used for qPCR (as listed in Table 1), with TATA-binding protein (TBP) serving as the reference gene.

The amplification protocol was as follows: initial denaturation at 95°C for 5 minutes, followed by 40 cycles of denaturation at 95°C for 10 seconds and primer annealing at 60°C for 30 seconds. Relative expression levels were normalized to the TBP reference gene expression. Ct and ΔΔCt values were calculated for each target gene relative to the control condition (control siRNA, no treatment) using QuantStudio™ Design and Analysis Software. Data analysis was conducted in Excel, and expression fold changes (2^−ΔΔCt values) were calculated.

2.4. Western blot

A total of 15 µg of protein from each lysate (corresponding to each experimental condition) was mixed with 5 µl of Laemmli buffer and boiled at 95°C for 5 minutes. The denatured samples, along with All-Blue Precision Plus Protein™ Standards (Bio-Rad Laboratories, Munich, Germany), were separated electrophoretically on a 4–12 % NuPAGE™ Bis-Tris SDS Gel (Invitrogen, Waltham, MA, USA). SDS-PAGE was run at a voltage between 80 and 110 volts until the individual protein bands were well-resolved within the molecular weight range of 250 kDa to 10 kDa or until the dye front reached the bottom of the gel.

The separated proteins were transferred onto a nitrocellulose membrane using the semi-dry transfer method with the Turbo-Blot Transfer

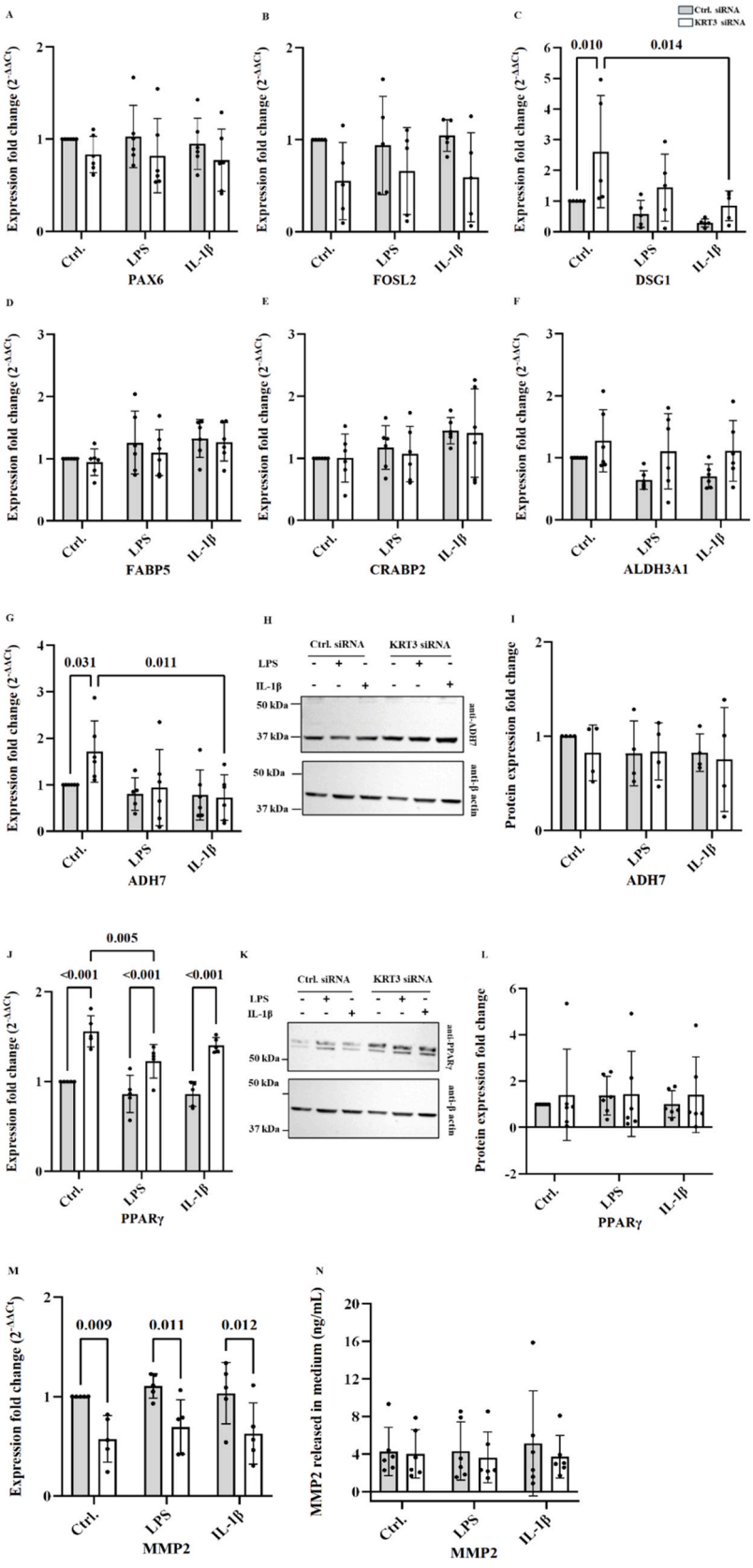

(caption on next page)

Fig. 3. Paired box protein 6 (PAX6), Fos-like antigen 2 (FOSL2), desmoglein 1 (DSG1), fatty acid-binding protein 5 (FABP5), cellular retinoic acid-binding protein 2 (CRABP2), aldehyde dehydrogenase 3 family member A1 (ALDH3A1), alcohol dehydrogenase 7 (ADH7), peroxisome proliferator-activated receptor gamma (PPARγ) and matrix metalloproteinase 2 (MMP2) mRNA and ADH7 and PPARγ protein levels in primary human limbal epithelial cells (LECs) and MMP2 protein levels in the cell culture medium 72 hours after transfection with control siRNA (grey) or with KRT3 knockdown siRNA (white), without or with lipopolysaccharide (LPS) or interleukin 1β (IL-1β) (A-J) ($n = 6$). Data are shown as mean ± SD. Statistical analysis has been performed using two-way ANOVA followed by Tukey test. Representative western blot images are also displayed (B). p values below 0.05 were considered statistically significant. PAX6, FOSL2, FABP5, CRABP2 and ALDH3A1 mRNA levels did not change significantly following KRT3 siRNA knockdown without or with LPS or IL-1β treatment ($p \geq 0.081$) (A, B, D-F). DSG1 and ADH7 mRNA levels were upregulated following KRT3 siRNA knockdown, without inflammatory conditions ($p = 0.010$; $p = 0.031$). IL-1β induced inflammation downregulated *DSG1* and *ADH7* mRNA levels in KRT3 siRNA knockdown LECs ($p = 0.014$; $p = 0.011$) (C, G). DSG1 protein could be detected in our positive control, but not in siRNA knockdown or siRNA controls LECs. ADH7 protein level did not change significantly after KRT3 siRNA knockdown, without or with inflammatory conditions ($p \geq 0.457$). KRT3 siRNA knockdown upregulated PPARγ mRNA levels without or with LPS or IL-1β induced inflammation ($p < 0.001$ for all). In LECs with KRT3 siRNA knockdown, LPS treatment upregulated PPARγ mRNA levels ($p = 0.005$). PPARγ protein level did not change significantly following siRNA KRT3 knockdown, without or with inflammatory conditions ($p \geq 0.607$) (H-J). KRT3 siRNA knockdown downregulated MMP2 mRNA levels without or with LPS or IL-1β induced inflammation ($p \leq 0.012$), without changes at MMP2 protein level in the cell culture supernatant ($p \geq 0.457$) (K-M).

System (Bio-Rad, Hercules, CA, USA). Transfer conditions were set at 25 volts and 1.3 amperes for 7 minutes. After the transfer, the membrane was washed three times with Froxx Wash Buffer, with each wash lasting 5 minutes. The membrane was then incubated with the primary antibody, prepared as per the dilutions noted in Table 2. Primary antibodies were diluted using the Western Blot Froxx Buffer Kit, which included a combined blocking buffer and secondary antibody solution (Bio Froxx GmbH, Einhausen, Germany).

For chemiluminescent signal detection, the membrane was incubated with Pierce™ ECL Western Blotting Substrate (Thermo Fisher Scientific, Pennsylvania, USA) for 5 minutes in the dark. Images were captured using the iBright™ 1500 Imaging System (Thermo Fisher Scientific, Pennsylvania, USA). For signal quantification of protein expression, densitometric analysis of western blot membranes was performed using iBright™ Analysis Software (Invitrogen, Waltham, Massachusetts, USA).

β-Actin was used as a loading control, and each Western blot was repeated five times for consistency.

2.5. ELISA

IL-6 and MMP2 concentrations in the cell culture supernatant were measured using the commercially available Human IL-6 DuoSet™ ELISA Kit (DY206–05) and the Human MMP2 DuoSet™ ELISA kit (DY902), from R&D Systems (Minneapolis, USA). Measurements were conducted according to the manufacturer's instructions, with all measurements performed in duplicate.

For the assay, 100 µl of the capture antibody was added to each well of a 96-well plate (High Binding ELISA-Plate, Sarstedt, Germany) and incubated overnight at room temperature. The plate was then washed three times with 400 µl of wash buffer (0.05 % Tween 20 in PBS) per well, followed by blocking with 300 µl of reagent diluent (1 % BSA in PBS). Next, 100 µl of the supernatant and the appropriate standards were added to each well and incubated for 2 hours. After another round of washing, 100 µl of detection antibody was added to each well and incubated.

Following further washing steps, the wells were incubated with 100 µl of streptavidin-HRP conjugate for 20 minutes. This was followed by additional washing and the addition of 100 µl of TMB substrate solution (3,3′,5,5′-tetramethylbenzidine, 1-Step Ultra TMB-ELISA Substrate Solution, Thermo Fisher, CA, USA) per well. The reaction was stopped by adding 50 µl of stop solution (2 N H_2SO_4) to each well.

The optical density (OD) was measured at 450 nm with optical correction at 540 nm using a Tecan Infinite 50 machine (Tecan Group AG, Männedorf, Switzerland) and Magellan software. OD values were used for statistical analyses and to calculate IL-6 and MMP2 concentrations using a non-linear data fit model.

2.6. Statistical analysis

GraphPad Prism, version 10.2.2 (San Diego, CA, USA), was used for statistical analysis. Outliers were identified using the online GraphPad Prism Outlier Calculator, which applies Grubbs' test (with a standard significance level of $\alpha = 0.05$). For the different treatment conditions following transfection, mRNA expression values (ΔΔCt) and relative protein expression levels were compared to controls using two-way ANOVA followed by Tukey's post hoc test. A p-value of less than 0.05 was considered statistically significant.

All experiments included at least $n = 6$ biological replicates. As our work is based on primary donor-derived cells, generating technical replicates was not feasible due to the limited availability of donor material for repeated experiments.

3. Results

3.1. KRT3 knockdown without and with inflammatory conditions

KRT3 mRNA expression exhibited a significant decrease after KRT3 siRNA knockdown when compared to siRNA controls, irrespective of the presence or absence of LPS-induced inflammation ($p \leq 0.0120$) (Fig. 2A). Likewise, KRT3 protein expression was markedly lower following KRT3 siRNA knockdown relative to siRNA controls, under both inflammatory and non-inflammatory conditions ($p \leq 0.002$) (Fig. 2 B, C). Moreover, in control siRNA-transfected cells, IL-1β-induced inflammation led to a notable reduction in KRT3 mRNA levels compared to non-inflamed conditions ($p = 0.005$). Additionally, KRT3 protein expression was significantly diminished in IL-1β-induced inflammation compared to LPS-induced inflammation within control siRNA-transfected cells ($p = 0.038$) (Fig. 2A-C).

3.2. KRT12, KRT13 and KRT19 levels without and with inflammatory conditions

The mRNA levels of *KRT12, KRT13*, and *KRT19* remained unchanged following KRT3 siRNA knockdown, regardless of whether LPS or IL-1β treatment was applied ($p \geq 0.085$) (Fig. 2D-F).

3.3. Transcription factors, retinoic acid signaling components and matrix metalloproteinase 2 (MMP2) levels without and with inflammatory conditions

The mRNA levels of *PAX6, FOSL2, FABP5, CRABP2*, and *ALDH3A1* remained unchanged following KRT3 siRNA knockdown, regardless of the presence or absence of LPS- or IL-1β-induced inflammation ($p \geq 0.081$) (Fig. 3 A, B, D-F).

In contrast, *DSG1* and *ADH7* mRNA levels were significantly upregulated after KRT3 siRNA knockdown under non-inflammatory conditions ($p = 0.010$; $p = 0.031$). However, in KRT3-knockdown LECs, IL-1β-induced inflammation led to a significant downregulation of *DSG1* and *ADH7* mRNA levels ($p = 0.014$; $p = 0.011$) (Fig. 3 C, G). At the protein level, DSG1 was detectable in our positive control, but not in either the siRNA knockdown or siRNA control LECs. Meanwhile, ADH7

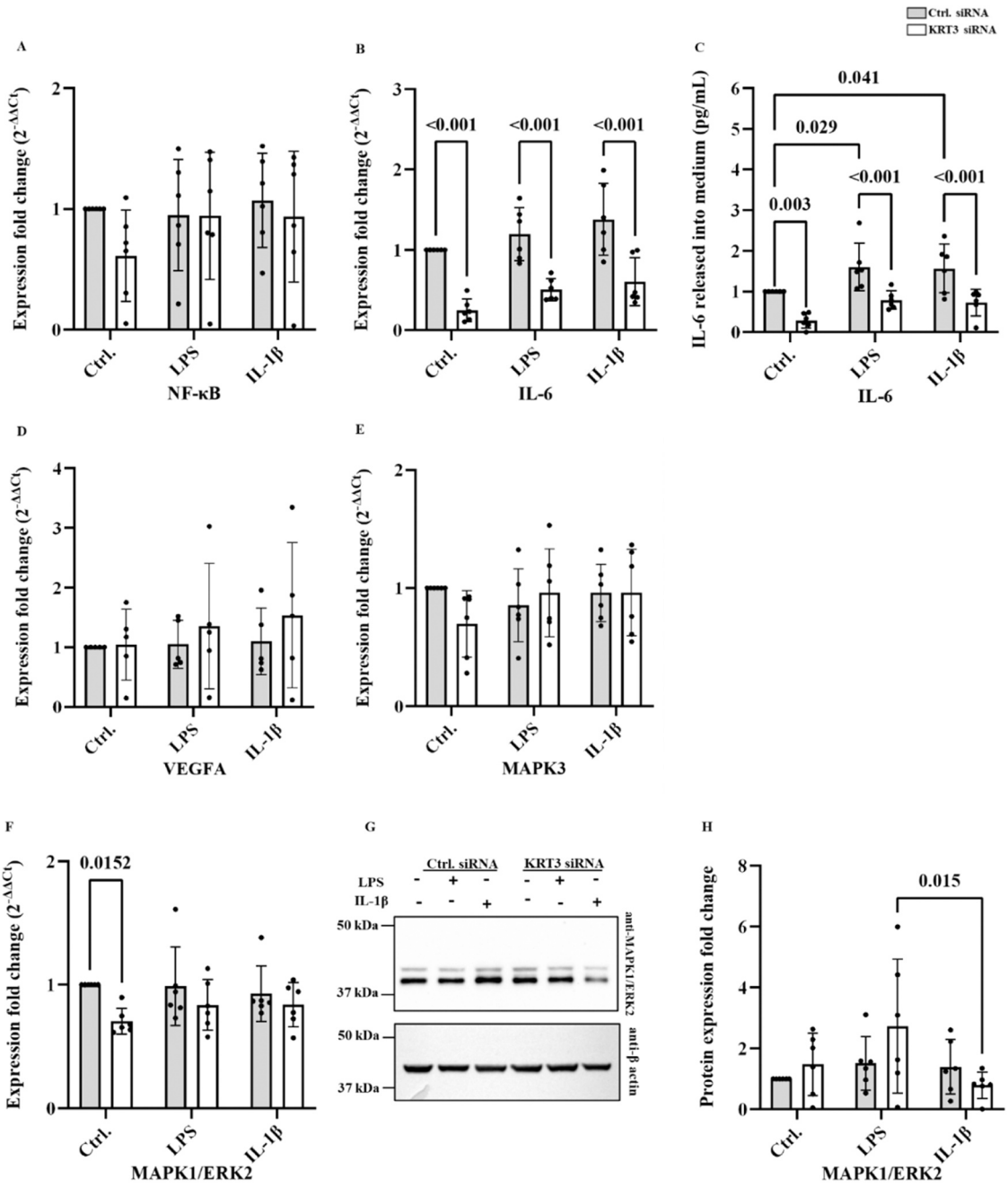

Fig. 4. Nuclear Factor kappa-light-chain-enhancer of activated B cells (NF-κB) mRNA levels, interleukin-6 (IL-6) mRNA and protein levels and vascular endothelial growth factor A (VEGFA), mitogen-activated protein kinase 3 (MAPK3) mRNA levels and mitogen-activated protein kinase 3/ Extracellular Signal-Regulated Kinase 2 mRNA and protein levels in primary human limbal epithelial cells (LECs) 72 hours after transfection with control siRNA (grey) or with KRT3 knockdown siRNA (white), without or with lipopolysaccharide (LPS) or interleukin 1β (IL-1β) (A-E) (n = 6). Data are shown as mean ± SD. Statistical analysis has been performed using two-way ANOVA followed by Tukey test. p values below 0.05 were considered statistically significant. KRT3 siRNA knockdown downregulated IL-6 mRNA and protein levels without or with LPS or IL-1β induced inflammation ($p \leq 0.003$) (B, C). In addition, in LECs following control siRNA knockdown, LPS and IL-1β induced inflammation upregulated IL-6 protein levels ($p = 0.029$; $p = 0.041$) (C). KRT3 knockdown also downregulated MAPK1 mRNA level without inflammatory stimuli ($p = 0.0152$) (E). ERK2 protein level was significantly lower in IL-1β induced inflammation, than in LPS induced inflammation, in KRT3 knockdown LECs ($p = 0.015$) (H). NF-κB, VEGFA and MAPK3 mRNA levels did not change significantly following KRT3 siRNA knockdown without or with LPS or IL-1β treatment ($p \geq 0.215$) (A, D, F).

protein levels remained unchanged after KRT3 knockdown, regardless of inflammatory conditions ($p \geq 0.457$).

KRT3 siRNA knockdown resulted in a significant upregulation of *PPARγ* mRNA levels, both in the absence and presence of LPS- or IL-1β-induced inflammation ($p < 0.001$ for all conditions). Furthermore, in KRT3-knockdown LECs, LPS treatment further increased *PPARγ* mRNA expression ($p = 0.005$). However, PPARγ protein levels were not significantly affected following KRT3 siRNA knockdown, regardless of inflammatory conditions ($p \geq 0.607$) (Fig. 3 H-J).

Additionally, *MMP2* mRNA expression was significantly downregulated following KRT3 siRNA knockdown, both without and with LPS- or IL-1β-induced inflammation ($p \leq 0.012$). However, no significant changes were observed in MMP2 protein levels in the cell culture supernatant ($p \geq 0.457$) (Fig. 3 K-M).

Table 3
List of antibodies used in Western blot analysis.

Antibody	Source	Molecular weight (kDa)	Catalog No./ Manufacturer	Dilution
β - Actin	Rabbit, polyclonal	42 kDa	81115–1-RR, Proteintech, USA.	1:10,000
ADH7	Rabbit, polyclonal	40 kDa	PA5–98484, Invitrogen.	1:500
ERK2/ MAPK1	Rabbit, polyclonal	44 – 42 kDa	#4695, Cell Signalling Technology, Massachusetts, USA.	1:1000
KRT3	Mouse, monoclonal	64 kDa	CBL218, Merk, Darmstadt, Germany	1:500
PPARγ	Rabbit polyclonal	50–60 kDa	166431AP, Proteintech, CA, USA.	1:500

3.4. Inflammatory and proangiogenic factor levels without and with inflammatory conditions

KRT3 knockdown via siRNA led to a reduction in both IL-6 mRNA and protein levels, regardless of the presence or absence of LPS- or IL-1β-induced inflammation ($p \leq 0.003$) (Fig. 4 A-C). Furthermore, in LECs treated with control siRNA, exposure to LPS or IL-1β resulted in an upregulation of IL-6 protein levels ($p = 0.029$; $p = 0.041$) (Fig. 4C).

Additionally, KRT3 knockdown caused a decrease in *MAPK1* mRNA levels in the absence of inflammatory stimulation ($p = 0.0152$). The ERK2 protein level was significantly lower in IL-1β-induced inflammation compared to LPS-induced inflammation in KRT3-knockdown LECs ($p = 0.015$) (Fig. 4 F, H). Conversely, the mRNA expression of *NF-κB*, *VEGFA*, and *MAPK3* remained unchanged following KRT3 siRNA knockdown, irrespective of LPS or IL-1β treatment ($p \geq 0.215$) (Fig. 4 A, D, E).Table 3.

4. Discussion

In this study, we explored the isolated *in vitro* effects of KRT3 knockdown in limbal epithelial cells and examined the combined impact of inflammation under conditions of KRT3 knockdown. The changes, which have been related to KRT3 levels without and with inflammatory conditions after 72 hours are summarised at Table 4**.** The most notable finding was that IL-6 expression was significantly downregulated at both the transcriptional and protein levels following KRT3 knockdown, also without and with inflammatory conditions. In contrast, in control siRNA-transfected LECs, without KRT3 knockdown, IL-1β-induced inflammation alone significantly reduced KRT3 mRNA and protein levels, while increasing IL-6 protein levels. This contrasts with the behaviour of KRT3 knockdown LECs.

This suggests that in normal LECs, inflammatory stimuli stimulate IL-6 production through a feedback loop. Notably, these regulatory mechanisms were absent in KRT3 knockdown LECs. As a result, even in the presence of inflammation, KRT3 knockdown LECs maintained the same level of inflammatory IL-6 protein secretion.

These findings highlight the distinct response of KRT3 knockdown LECs to inflammatory conditions, uncovering their inability to engage in the feedback mechanisms typically observed in normal LECs. Chronic ocular surface inflammation is a characteristic feature of PAX6 halpoinsufficiency-related congenital aniridia, where the downstream KRT3 levels are also downregulated (L. Latta et al., 2021). Therefore, in congenital aniridia (PAX6 knockdown) LECs, we propose that LECs are unable to adjust their differentiation processes or modulate IL-6 secretion in response to inflammatory stimuli. This seems to be related to KRT3 knockdown.

Interestingly, in an indirect co-culture analysis of normal and aniridia (PAX6-knockdown) LECs and limbal fibroblast cells (LFCs), treating aniridia LFCs with conditioned medium from normal LECs significantly increased IL-6 protein levels. In contrast, treatment of the same cells with conditioned medium from PAX6-knockdown LECs did not result in any significant changes in the expression of inflammatory biomarkers (Berger et al., 2024). This suggests that in congenital aniridia, the inflammatory response is impaired not only in LECs but also in LFCs, which may collectively contribute to the development and progression of aniridia-associated keratopathy.

Our results suggest that in Meesmann epithelial corneal dystrophy with KRT3 knockdown, IL-6 protein levels are downregulated in LECs, even in the absence of inflammation. Furthermore, in response to external inflammatory stimuli, the IL-6 secretion response appears to be absent. These alterations are likely linked to the known epithelial changes and the subsequent disruption of epithelial-stromal interactions observed in MECD (Szaflik et al., 2008; Chen et al., 2015; Cao et al., 2013). Nevertheless, these need further evaluation, especially regarding the interactions with the corneal stromal cells.

Interestingly, we did not observe any change in KRT12 expression after KRT3 knockdown, despite its well-established role as the heterodimeric partner of KRT3 in maintaining corneal epithelial identity. The underlying reasons for this finding remain unclear and warrant further investigation.

KRT13 and KRT19 mRNA levels remained unchanged following KRT3 knockdown and/or exposure to inflammatory stimuli. This indicates that the applied conditions do not promote a shift of LECs towards a conjunctival epithelial phenotype characterized by KRT13 and KRT19 expression (Lorenz Latta et al., 2021; Ramirez-Miranda et al., 2011).

KRT3 knockdown at the protein level also resulted in transcriptional upregulation of DSG1, ADH7, and PPARγ, along with downregulation of MAPK1. After KRT3 siRNA knockdown, LPS-induced inflammation reduced PPARγ mRNA levels, while IL-1β-induced inflammation decreased DSG1 and ADH7 mRNA levels. These changes, however, did

Table 4
Significant effects of KRT3 knockdown in primary human limbal epithelial cells (LECs) 72 hours post-transfection, with and without lipopolysaccharide (LPS) or interleukin-1β (IL-1β)-induced inflammation, compared to control siRNA treatment without or with the same inflammatory condition. The table summarizes significant changes observed at both the transcriptional and translational levels.

	KRT3 knockdown	KRT3 knockdown+ LPS	KRT3 knockdown + IL-1β	KRT3 knockdown	KRT3 knockdown + LPS	KRT3 knockdown + IL-1β
	mRNA			**Protein**		
KRT3	**↓ ($p < 0.001$)**	**↓ ($p = 0.012$)**	n.s.	**↓ ($p = 0.002$)**	**↓ ($p < 0.001$)**	n.s.
DSG1	**↑ ($p = 0.010$)**	n.s.	n.s.	-	-	-
ADH7	**↑ ($p = 0.031$)**	n.s.	n.s.	n.s.	n.s.	n.s.
PPARγ	**↑ ($p < 0.001$)**	**↑ ($p < 0.001$)**	**↑ ($p < 0.001$)**	n.s.	n.s.	n.s.
MMP2	**↓ ($p = 0.009$)**	**↓ ($p = 0.011$)**	**↓ ($p = 0.012$)**	n.s.	n.s.	n.s.
IL−6	**↓ ($p < 0.001$)**	**↓ ($p < 0.001$)**	**↓ ($p < 0.001$)**	**↓ ($p = 0.003$)**	**↓ ($p < 0.001$)**	**↓ ($p < 0.001$)**
MAPK1/ ERK2	**↓ ($p = 0.015$)**	n.s.	n.s.	n.s.	n.s.	n.s.

Although KRT3 knockdown at both the mRNA and protein levels led to significant changes in the mRNA expression of *DSG1, ADH7, PPARγ, MMP2*, and *MAPK1/ERK2*, a corresponding significant change at both the mRNA and protein levels was observed only for IL-6 at the 72-hour time point.
n.s. = not significant

not affect the protein levels. Interestingly, these inflammatory stimuli appeared to restore DSG1, ADH7, and PPARγ mRNA levels in KRT3 knockdown LECs to their baseline levels (as observed before knockdown). These findings may suggest a corresponding dysregulation of components within the retinoic acid pathway as a result of KRT3 dysregulation, as well as the existence of a potential feedback loop in retinoic acid signaling. Previous studies have also reported direct downregulation of DSG1 and KRT3 in LECs, in response to retinoic acid treatment, which may also explain these observations (Lorenz Latta et al., 2021; 2019). In addition, in PAX6-halpoinsufficiency associated congenital aniridia the downregulation of retinol-metabolizing enzymes, such as ADH7 and ALDH3A1, has been reported in both LECs and CECs (Lorenz Latta et al., 2021).

PPARγ knockdown in LECs via siRNA has been shown to regulate KRT3 transcription. As a nuclear receptor, PPARγ can activate the retinoic acid pathway. In murine models lacking PPARγ, reduced levels of KRT3, KRT12, and KRT15 have been observed, a finding supported by qPCR, immunohistochemistry, and protein expression studies (Meyer et al., 2015). Conversely, in our study, PPARγ mRNA levels were upregulated in all KRT3 siRNA knockdown cells, yet no corresponding changes were detected at the protein level, regardless of inflammatory treatment. This observation suggests that downstream targets may also play a role in regulating transcription factors themselves. As transcription factors influence downstream targets, it is possible that feedback mechanisms exist, where downstream targets, in turn, modulate transcription factor activity.

The MAPK/ERK pathway is a critical mitogen-activated signalling cascade that regulates various functions associated with PAX6-induced aniridia pathways (Leiper et al., 2006). Upon KRT3 knockdown, MAPK1 mRNA levels were reduced; however, inflammation restored these levels. Notably, under the same conditions, no changes were observed at ERK protein level (Fig. 4). Nevertheless, in KRT3 knockdown LECs, ERK protein levels following IL-1β induced inflammation were lower, than after LPS induced inflammation. KRT3 knockdown alone does not appear to significantly affect the MAPK/ERK pathway, either in the absence or presence of inflammatory conditions.

Limbal stem cells in the corneal tissue give rise to LECs, which differentiate and migrate centripetally toward the central corneal epithelium, where they mature into central corneal epithelial cells (CECs). This process plays a critical role in corneal epithelial cell renewal and regeneration. The continuous cycle of epithelial cell differentiation and migration is essential for maintaining the healthy transparency of the corneal tissue. Keratins, particularly KRT3 and KRT12, serve as essential differentiation markers of the corneal epithelium. The relative expression of keratins in LECs is quantitatively lower compared to differentiated CECs (Rubelowski et al., 2020; Latta et al., 2018a). Congenital aniridia patients lack the cytokeratins KRT3 and KRT12 in their LECs. In aniridia patients, progressive limbal stem cell deficiency, a loss of corneal transparency and neovascularisation are hallmark symptoms of the disease and the related AAK. Based on our current study, PAX6 downstream KRT3 knockdown in congenital aniridia LECs lack IL-6 secretion adaptation in response to inflammation. This highlights the critical role of KRT3 knockdown as a key factor contributing to the development and progression of aniridia-associated keratopathy.

Clinically, aberrant KRT3 expression may serve as a diagnostic tool to monitor AAK progression. KRT3, along with KRT12, is a crucial marker of terminal differentiation in corneal epithelial cells, and its expression also signifies successful regeneration in limbal stem cell transplantation, particularly in conditions like AAK. Furthermore, targeted modulation of KRT3, for example via CRISPR/Cas9, may influence cell fate decisions and improve the outcomes of stem cell-based therapies for corneal diseases with KRT3 knockdown. Furthermore, from a therapeutic perspective, the use of anti-inflammatory eye drops or IL-6 pathway modulators, such as IL-6 receptor antagonists, may help to suppress inflammation in patients with impaired KRT3 expression, for example in patients with *PAX6* pathogenic variant related congenital aniridia or Meesmann corneal dystrophy.

A limitation of our study is that in vitro culture conditions do not permit investigation of the long-term effects of KRT3 knockdown and cannot fully replicate the complexity of gene networks, molecular interactions, and signalling pathways present in in vivo systems. These aspects warrant further exploration in animal models, under both physiological and inflammatory conditions. Additionally, for the differentiation markers DSG1, ADH7, and the transcription factor PPARγ, we observed changes at the transcriptional level, but not at the protein level. Understanding the underlying mechanisms behind this discrepancy, including the analysis of regulatory networks, would greatly benefit from longer-term in vivo studies.

In summary, in normal LECs, inflammatory stimuli induce IL-6 production. These mechanisms are absent in KRT3 knockdown LECs. As a result, despite the presence of inflammation, KRT3 knockdown LECs maintain their inflammatory IL-6 protein secretion. Longer-term studies, including the use of in vivo models, may help elucidate the underlying mechanisms and associated changes in regulatory networks.

CRediT authorship contribution statement

Hsu Shao-Lun: Writing – review & editing. **Liu Shanhe:** Writing – review & editing. **Szentmáry Nóra:** Writing – review & editing, Visualization, Supervision, Software, Resources, Project administration, Methodology, Conceptualization. **Suiwal Shweta:** Writing – review & editing. **Seitz Berthold:** Writing – review & editing. **Fries Fabian:** Writing – review & editing. **Li Shuailin:** Writing – review & editing. **Li Zhen:** Writing – review & editing. **Amini Maryam:** Writing – review & editing, Visualization, Supervision, Software, Project administration, Methodology, Data curation, Conceptualization. **Kundu Swarnali:** Writing – original draft, Visualization, Validation, Software, Project administration, Methodology, Investigation, Formal analysis, Data curation, Conceptualization. **Stachon Tanja:** Writing – review & editing, Visualization, Supervision, Software, Project administration, Methodology, Data curation, Conceptualization.

Ethical statement

Our study was approved by the Ethical Committee of Saarland/Germany (no. 162/23). Written informed consent was obtained from all participants or their relatives. In all the experiments described henceforth, the human donor tissues were handled according to the Declaration of Helsinki principles.

Declaration of Competing Interest

The authors have no conflicts to disclose relevant to the production and publication of this work.

Acknowledgements

The work of Swarnali Kundu, Maryam Amini, Tanja Stachon, Fabian Fries, Zhen Li, Shuailin Li, Shanhe Liu, Shao-Lun Shu, Shweta Suiwal and Nóra Szentmáry at the Dr. Rolf M. Schwiete Center for Limbal Stem Cell and Congenital Aniridia Research has been supported by the Dr. Rolf M. Schwiete Foundation. The work of Zhen Li and Shanhe Liu has been supported by the China Scholarship Council.

References

Berger, M., Szentmáry, N., Berger, T., Seitz, B., Fries, F.N., Suiwal, S., Amini, M., Stachon, T., 2024. Reciprocal effects of conditioned medium on gene and protein expression of limbal epithelial cells and limbal fibroblasts in congenital aniridia. Ophthalmology 121 (2), 243.

Cao, W., Yan, M., Hao, Q., Wang, S., Wu, L., Liu, Q., Li, M., Biddle, F.G., Wu, W., 2013. Autosomal-dominant meesmann epithelial corneal dystrophy without an exon

mutation in the Keratin-3 or Keratin-12 gene in a chinese family. J. Int. Med. Res. 41 (2), 511–518. https://doi.org/10.1177/0300060513477306.
Chen, J.L., Lin, B.R., Gee, K.M., Gee, J.A., Chung, D.-W.D., Frausto, R.F., Deng, S.X., Aldave, A.J., 2015. Identification of presumed pathogenic KRT3 Und KRT12 gene mutations associated with meesmann corneal dystrophy. Mol. Vis. (21), 1378–1386.
Cunha, D.L., Arno, G., Corton, M., Moosajee, M., 2019. The spectrum of PAX6 mutations and genotype-phenotype correlations in the eye. Genes 10, *1050*. https://doi.org/10.3390/GENES10121050. ⟨https://www.mdpi.com/2073-4425/10/12/1050/htm⟩.
Dias, P.M., Banerjee, G., 2013. The Role of Th17/IL-17 on Eosinophilic Inflammation. J. Autoimmun. 40 (1), 9–20. https://doi.org/10.1016/j.jaut.2012.07.004.
Ihnatko, R., Eden, U., Fagerholm, P., Lagali, N., 2022. Congenital aniridia and the ocular surface. accessed September 9 Ocul. Surf. 14 (2), 196–206. https://doi.org/10.1016/J.JTOS.2015.10.003. ⟨https://pubmed.ncbi.nlm.nih.gov/26738798/⟩. accessed September 9.
Ihnatko, R., Edén, U., Lagali, N., Dellby, A., Fagerholm, P., 2013. Analysis of protein composition and protein expression in the tear fluid of patients with congenital aniridia. J. Proteom. 94, 78–88. https://doi.org/10.1016/j.jprot.2013.09.003.
Irvine, A.D., Corden, L.D., Swensson4, O., Swenssons, B., Moore, J.E., Frazer, D.G., Smith, F.J.D., et al., Mutations in Cornea-Specific Keratin K3 or K12 Genes Cause Meesmann's Corneal Dystrophy, 1997.
Kao, W., Converse, R.L., Shiraishi, A., Kao, C., Ishizaki, M., Doetschman, T., Duffy, J., 1996. Keratin 12-Deficient Mice Have Fragile Corneal Epithelia 13 (37), 2572–2584.
Karantza, V., 2011. Keratins in health and cancer: more than mere epithelial cell markers. Oncogene.
Katiyar, P., Stachon, T., Fries, F.N., Parow, F., Ulrich, M., Langenbucher, A., Cayless, A., et al., 2022. Decreased FABP5 and DSG1 protein expression following PAX6 knockdown of differentiated human limbal epithelial cells. Exp. Eye Res. 215. https://doi.org/10.1016/j.exer.2021.108904.
Kiselev, Y., Andersen, S., Johannessen, C., Fjukstad, B., Standahl Olsen, K., Stenvold, H., Al-Saad, S., et al., 2018. Transcription factor PAX6 as a novel prognostic factor and putative tumour suppressor in non-small cell lung cancer. Sci. Rep. 8 (1), 5059. https://doi.org/10.1038/s41598-018-23417-z.
Kitazawa, K., Hikichi, T., Nakamura, T., Sotozono, C., Kinoshita, S., Masui, S., 2017. PAX6 Regulates human corneal epithelium cell identity. Exp. Eye Res. 154, 30–38. https://doi.org/10.1016/j.exer.2016.11.005.
Landsend, E.C.S., Utheim, Ø.A., Pedersen, H.R., Aass, H.C.D., Lagali, N., Dartt, D.A., Baraas, R.C., Utheim, T.P., 2018. The level of inflammatory tear cytokines is elevated in congenital aniridia and associated with meibomian gland dysfunction. Invest. Ophthalmol. Vis. Sci. 59 (5), 2197–2204. https://doi.org/10.1167/iovs.18-24027.
Latta, L., Figueiredo, F.C., Ashery-Padan, R., Collinson, J.M., Daniels, J., Ferrari, S., Szentmáry, N., et al., 2021. Pathophysiology of aniridia-associated keratopathy: developmental aspects and unanswered questions. Ocul. Surf.
Latta, Lorenz, Knebel, I., Bleil, C., Stachon, T., Katiyar, P., Zussy, C., Fries, F.N., Käsmann-Kellner, B., Seitz, B., Szentmáry, N., 2021. Similarities in DSG1 and KRT3 down regulation through retinoic acid treatment and PAX6 knockdown related expression profiles: does PAX6 Affect RA signaling in limbal epithelial cells? Biomolecules 11 (11). https://doi.org/10.3390/biom11111651.
Latta, Lorenz, Nordström, K., Stachon, T., Langenbucher, A., Fries, F.N., Szentmáry, N., Seitz, B., Käsmann-Kellner, B., 2019. Expression of retinoic acid signaling components ADH7 and ALDH1A1 is reduced in aniridia limbal epithelial cells and a sirna primary cell based aniridia model. Exp. Eye Res. 179, 8–17. https://doi.org/10.1016/j.exer.2018.10.002.
Latta, Lorenz, Viestenz, A., Stachon, T., Colanesi, S., Szentmáry, N., Seitz, B., Käsmann-Kellner, B., 2018a. Human aniridia limbal epithelial cells lack expression of Keratins K3 and K12. Exp. Eye Res. 167, 100–109. https://doi.org/10.1016/j.exer.2017.11.005.
Latta, Lorenz, Viestenz, A., Stachon, T., Colanesi, S., Szentmáry, N., Seitz, B., Käsmann-Kellner, B., 2018b. Human aniridia limbal epithelial cells lack expression of keratins K3 and K12. Exp. Eye Res. 167, 100–109. https://doi.org/10.1016/j.exer.2017.11.005.
Leiper, L.J., Walczysko, P., Kucerova, R., Ou, J., Shanley, L.J., Lawson, D., Forrester, J.V., McCaig, C.D., Zhao, M., Collinson, J.M., 2006. The roles of calcium signaling and ERK1/2 phosphorylation in a Pax6+ /- mouse model of epithelial wound-healing delay. BMC Biol. 4. https://doi.org/10.1186/1741-7007-4-27.
Li, W., Chen, Y.T., Hayashida, Y., Blanco, G., Kheirkah, A., He, H., Chen, S.Y., Liu, C.Y., Tseng, S.C.G., 2008. Down-regulation of Pax6 Is associated with abnormal differentiation of corneal epithelial cells in severe ocular surface diseases. J. Pathol. 214 (1), 114–122. https://doi.org/10.1002/path.2256.
Mall, R., Franke, W.W., Schiller, D.L., Geiger, B., Krepler, R., 1982. The catalog of human cytokeratins: patterns of expression in normal epithelia, tumors and cultured cells review. Cell 31 (1).
Meyer, E.A., Call, M., Zenkel, M., Polisetti, N., Kruse, F.E., Kao, W., Schlotzer-Schrehardt, U., 2015. Corneal epithelial homeostasis: the importance of the transcription factor PPARG. Invest. Ophthalmol. Vis. Sci. 56 (7), 5647.
Ouyang, H., Xue, Y., Lin, Y., Zhang, X., Xi, L., Patel, S., Cai, H., et al., 2014. WNT7A and PAX6 Define Corneal Epithelium Homeostasis and Pathogenesis. Nature 511 (7509), 358–361. https://doi.org/10.1038/nature13465.
Page, M.J., Kell, D.B., Pretorius, E., 2022. The role of lipopolysaccharide-induced cell signalling in chronic inflammation. Chronic Stress.
Primiani, C.T., Ryan, V.H., Rao, J.S., Cam, M.C., Ahn, K., Modi, H.R., Rapoport, S.I., 2014. Coordinated gene expression of neuroinflammatory and cell signaling markers in dorsolateral prefrontal cortex during human brain development and aging. PLoS ONE 9 (10). https://doi.org/10.1371/journal.pone.0110972.
Ramaesh, T., Collinson, J.M., Ramaesh, K., Kaufman, M.H., West, J.D., Dhillon, B., 2003. Corneal abnormalities in Pax6+ /- small eye mice mimic human aniridia-related keratopathy. Invest. Ophthalmol. Vis. Sci. 44 (5), 1871–1878. https://doi.org/10.1167/iovs.02-0576.
Ramaesh, K., Ramaesh, T., Dutton, G.N., Dhillon, B., 2005. Evolving concepts on the pathogenic mechanisms of aniridia related keratopathy. Int. J. Biochem. Cell Biol.
Ramirez-Miranda, A., Nakatsu, M.N., Zarei-Ghanavati, S., Nguyen, C.V., Deng, S.X., 2011. Keratin 13 Is. a More Specif. Marker Conjunctival Epithelium Keratin 19.
Reeve, A.J., Patel, S., Fox, A., Walker, K., Urban, L., 2000. Intrathecally administered endotoxin or cytokines produce allodynia, hyperalgesia and changes in spinal cord neuronal responses to nociceptive stimuli in the rat. Eur. J. Pain. 4 (3), 247–257. https://doi.org/10.1053/eujp.2000.0177.
Rubelowski, A.K., Latta, L., Katiyar, P., Stachon, T., Käsmann-Kellner, B., Seitz, B., Szentmáry, N., 2020. HCE-T cell line lacks cornea-specific differentiation markers compared to primary limbal epithelial cells and differentiated corneal epithelium. Graefe's. Arch. Clin. Exp. Ophthalmol. 258 (3), 565–575. https://doi.org/10.1007/s00417-019-04563-0.
Sasamoto, Y., Hayashi, R., Park, S.J., Saito-Adachi, M., Suzuki, Y., Kawasaki, S., Quantock, A.J., Nakai, K., Tsujikawa, M., Nishida, K., 2016. PAX6 Isoforms, along with Reprogramming Factors, Differentially Regulate the Induction of Cornea-Specific Genes. Sci. Rep. 6, 20807. https://doi.org/10.1038/srep20807.
Schlötzer-Schrehardt, U., Latta, L., Gießl, A., Zenkel, M., Fries, F.N., Käsmann-Kellner, B., Kruse, F.E., Seitz, B., 2021. Dysfunction of the limbal epithelial stem cell niche in aniridia-associated keratopathy: limbal niche in aniridia-associated keratopathy. Ocul. Surf. 21, 160–173. https://doi.org/10.1016/j.jtos.2021.06.002.
Simmons, K.T., Xiao, Y., Pflugfelder, S.C., Paiva, C.S. de, 2016. Inflammatory response to lipopolysaccharide on the ocular surface in a murine dry eye model. Invest. Ophthalmol. Vis. Sci. 57 (6), 2443–2451. https://doi.org/10.1167/iovs.15-18396.
Szaflik, J.P., Ołdak, M., Maksym, R.B., Kamińska, A., Pollak, A., Udziela, M., Płoski, R., and Szaflik, J., Genetics of Meesmann Corneal Dystrophy: A Novel Mutation in the Keratin 3 Gene in an Asymptomatic Family Suggests Genotype-Phenotype Correlation, 2008.
Yücel, G., Zhao, Z., El-Battrawy, I., Lan, H., Lang, S., Li, X., Buljubasic, F., et al., 2017. Lipopolysaccharides induced inflammatory responses and electrophysiological dysfunctions in human-induced pluripotent stem cell derived cardiomyocytes. Sci. Rep. 7 (1). https://doi.org/10.1038/s41598-017-03147-4.